

Advanced Research Center for Beam Science – Electron Microscopy and Crystal Chemistry –

<http://eels.kuicr.kyoto-u.ac.jp/EMCC/home-en.html>



Prof
KURATA, Hiroki
(D Sc)



Assoc Prof
HARUTA, Mitsutaka
(D Sc)



Assist Prof
NEMOTO, Takashi
(D Sc)



Program-Specific Res*
OGAWA, Tetsuya
(D Sc)



Program-Specific Res*
KIYOMURA, Tsutomu

*Nanotechnology Platform

Researcher (pt)

YAMAGUCHI, Atsushi

Students

LAI, Ming Wei (D3)

IWASHIMIZU, Chisaki (D1)

KAWAGUCHI, Tomoki (M2)

Scope of Research

We study crystallographic and electronic structures of materials and their transformations through direct imaging of atoms or molecules by high-resolution electron spectromicroscopy, which realizes energy-filtered imaging and electron energy-loss spectroscopy as well as high-resolution imaging. By combining this with scanning probe microscopy, we cover the following subjects: 1) direct structure analysis, electron crystallographic analysis, 2) elemental analysis and electronic states analysis, 3) structure formation in solutions, and 4) epitaxial growth of molecules.



KEYWORDS

STEM-EELS ELNES Brownmillerite CTM4XAS Crystal Field Multiplet Calculation

Selected Publications

Saito, H.; Kurata, H., Formation of a Hybrid Plasmonic Waveguide Mode Probed by Dispersion Measurement, *J. Appl. Phys.*, **117**, [133107-1]-[133107-7] (2015).

Haruta, M.; Hosaka, Y.; Ichikawa, N.; Saito, T.; Shimakawa, Y.; Kurata, H., Determination of Elemental Ratio in an Atomic Column by Electron Energy-Loss Spectroscopy, *ACS Nano*, **10**, 6680-6684 (2016).

Haruta, M.; Fujiyoshi, Y.; Nemoto, T.; Ishizuka, A.; Ishizuka, K.; Kurata, H., Atomic-Resolution Two-Dimensional Mapping of Holes in the Cuprate Superconductor $\text{La}_{2-x}\text{Sr}_x\text{CuO}_{4+\delta}$, *Phys. Rev. B*, **97**, [205139-1]-[205139-5] (2018).

Yamaguchi, A.; Haruta, M.; Nemoto, T.; Kurata, H., Probing Directionality of Local Electronic Structure by Momentum-Selected STEM-EELS, *Appl. Phys. Lett.*, **113**, [053101-1]-[053101-4] (2018).

Haruta, M.; Fujiyoshi, Y.; Nemoto, T.; Ishizuka, A.; Ishizuka, K.; Kurata, H., Extremely Low Count Detection for EELS Spectrum Imaging by Reducing CCD Read-out Noise, *Ultramicroscopy*, **207**, [112827-1]-[112827-6] (2019).

Extraction of the Local Coordination and Electronic Structures of FeO₆ Octahedra Using Crystal Field Multiplet Calculations Combined with STEM-EELS

The material properties of metal oxides are sensitive to cation doping. The local atomic structure around such doped cations will be different from that in the bulk. The present work explores the extraction of the local structure of a minority component contained in an atomic column by analyzing the Fe $L_{2,3}$ energy-loss near-edge structure (ELNES) of atomic-resolution monochromated electron energy-loss spectra (EELS) using crystal field multiplet (CFM) calculations by CTM4XAS program. The present study focused on brownmillerite-type compounds, which have a structure $A_2BB'O_5$ comprising alternating layers of BO_4 tetrahedra and $B'O_6$ octahedra.

Figure 1 shows the experimental and simulated Fe $L_{2,3}$ -ELNES acquired from several iron oxide materials. These spectra show different features reflecting variations in local electronic structures. The energy levels of the $3d$ state for a transition metal having D_{4h} distorted octahedral symmetry in the mean field approximation is described by the crystal field parameters Dq , Dt , and Ds in CTM4XAS. In the present research, the energy width between two peaks in the experimental L_3 spectrum was employed as the crystal field splitting (CFS) $\Delta E = E_{d_{x^2-y^2}} - E_{d_{yzd_{zx}}} = 10Dq + 3Ds - 5Dt$. The optimal crystal field parameters were decided by fitting between simulated and experimental spectra. Figure 2 presents a calculated energy diagram of the Fe $3d$ state at an octahedral site. As for $Ca_2Fe_2O_5$ (CFO) and $Sr_2Fe_2O_5$ (SFO), the diagram roughly agrees with the one calculated by density functional theory (DFT). We can obtain reliable information concerning CFS with atomic-level resolution from experimental spectra in conjunction with CFM calculations without using DFT. In addition, the crystal field parameters are related to the $B'-O$ bond lengths: $Dq = Ze^2\langle r^4 \rangle / (6a^5)$, $Ds = (2/21)Ze^2\langle r^4 \rangle (1/a^5 - 1/b^5)$, where a and b are the equatorial and axial $B'-O$ bond lengths, r is the coordinate of the d electron. The bond lengths were estimated by using the $Ze^2\langle r^4 \rangle$ value derived from the Dq ($\Delta E = 10Dq = 1.4$ eV) and the bond length (2.02 Å) of α - Fe_2O_3 . The aspect ratios were estimated without using $Ze^2\langle r^4 \rangle$: $b/a = (4Dq / (4Dq - 7Dt))^{1/5}$. Table I compares the bond lengths and the aspect ratios determined by neutron diffraction and EELS. The aspect ratios obtained from the EELS data correspond reasonably well to the neutron data. The present method can reproduce not only CFS with atomic resolution but also local bond lengths of octahedra in real space.

We subsequently applied the same analysis to the Fe

$L_{2,3}$ ELNES acquired from the octahedral B' sites in $Ca_2Fe_{1.07}Mn_{0.93}O_5$ (CFMO), where the atomic concentration of Fe was $14.4 \pm 0.2\%$. In such cases, the local structure for the FeO_6 octahedra will be different from that for the more common MnO_6 . The aspect ratio is close to that for CFO although the bond lengths are different. The difference is significant because the neutron results primarily reflect the MnO_6 octahedra. In contrast, the EELS results show the unique local structure of the FeO_6 octahedra present as a minor component in B' site. Thus, it is demonstrated that the present method is effective for investigating local structures around impurities.

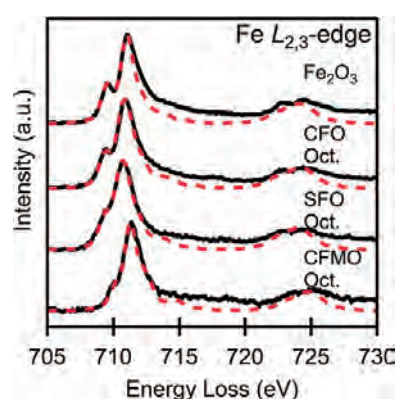


Figure 1. Fe $L_{2,3}$ -edge spectra acquired from α - Fe_2O_3 , $Ca_2Fe_2O_5$, $Sr_2Fe_2O_5$, and $Ca_2Fe_{1.07}Mn_{0.93}O_5$. Solid and dotted lines indicate experimental and simulated spectra, respectively. The energy range of fitting was 707–711.5 eV because the simulated spectra did not include the transitions to $4s$ and continuum states.

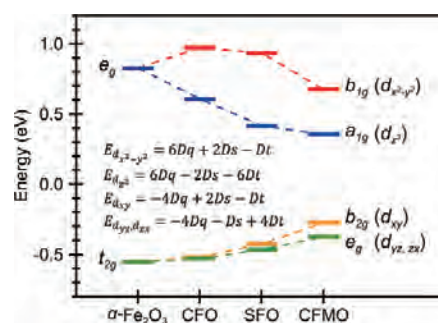


Figure 2. Energy diagram for the crystal field splitting of the Fe $3d$ state at an octahedral site.

Table I. The bond lengths obtained for various octahedra.

Sample	Bond	Neutron (Å)	EELS (Å)	Relative error (%)
$Ca_2Fe_2O_5$	a	1.97	2.00	1.4
	b	2.13	2.18	2.3
	b/a	1.08	1.09	1.0
$Sr_2Fe_2O_5$	a	1.98	2.04	2.8
	b	2.22	2.35	5.8
	b/a	1.12	1.16	3.6
$Ca_2Fe_{1.07}Mn_{0.93}O_5$	a	1.92	2.19	
	b	2.21	2.34	
	b/a	1.15	1.07	